# Even Hard-Sphere Colloidal Suspensions Display Fickian Yet Non-Gaussian Diffusion

Juan Guan,[†] Bo Wang,[†] and Steve Granick[†,‡,§,*]

[†]Departments of Materials Science, [‡]Chemistry, and [§]Physics, University of Illinois, Urbana, Illinois 61801, United States

ABSTRACT We scrutinize three decades of probability density displacement distribution in a simple colloidal suspension with hard-sphere interactions. In this index-matched and density-matched solvent, fluorescent tracer nanoparticles diffuse among matrix particles that are eight times larger, at concentrations from dilute to concentrated, over times up to when the tracer diffuses a few times its size. Displacement distributions of tracers, Gaussian in pure solvent, broaden systematically with increasing obstacle density. The onset of non-Gaussian dynamics is seen in even modestly dilute suspensions, which traditionally would be assumed to follow classic Gaussian expectation. The findings underscore, in agreement with recent studies of more esoteric soft matter systems, the prevalence of non-Gaussian yet Fickian diffusion.
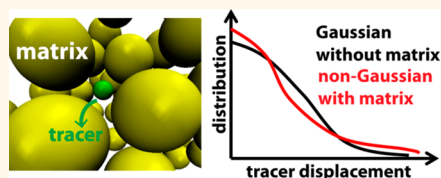
KEYWORDS: hard-sphere colloids · crowding · diffusion · complex fluids · non-Gaussian

Evidence is mounting of Fickian yet non-Gaussian Brownian diffusion in multiple systems.[1−9] In other words, even though it is commonly presumed that the random displacements that objects undergo during Brownian motion follow a normal (Gaussian) distribution, it has been observed that displacement distribution can be non-Gaussian when the mean square displacement remains linear in time. This is counterintuitive, as it seems to contradict the predicted Gaussian behavior at long times but has been reported repeatedly in independent systems: particles diffusing on phospholipid tubules,[1] particles diffusing in entangled actin,[1] liposomes diffusing in entangled actin,[2] polymer chains diffusing on a surface,[3,4] and particles diffusing among swimming cells.[5] A theoretical rationale has been provided that heterogeneity not sufficiently averaged out on a short time and length scale might underpin this behavior.[2] But a limitation of the experimental studies is that they concerned unusual systems with complicated specific interactions, making their generality difficult to assess.

Seeking to test the idea in a system more generally representative, we have designed the following experiments involving colloidal suspensions, with several considerations in mind. First, as specific interactions can introduce heterogeneity and interfere with diffusion, we sought to achieve hard-sphere interactions. Perfect hard-sphere behavior is now recognized impossible to fully realize in the laboratory, but the system we selected appears to come as close to this as can be done.[10,11] Second, to emulate the locally varying microenvironments that have been hypothesized to underpin this behavior,[2] we sought to work in suspensions whose concentration could be varied over a wide range. To implement this, we track with nanometer resolution the trajectories of colloidal-sized tracer particles embedded in a suspension of larger matrix particles (Figure 1a). The particle−particle interactions are simply hard sphere and hydrodynamic. The size ratio of 1:8 allows smaller particles to diffuse through the interstices between larger particles, no matter how closely the larger ones are packed. Evaluating displacement distribution over three decades in probability, we show non-Gaussian behavior while the diffusion is Fickian. Hydrodynamic interactions have been proposed to differ from spot to spot in crowded colloidal environments,[12,13] which might present heterogeneity to moving particles as they diffuse and lead to non-Gaussian displacement, although the underlying mechanism would differ from conventional glassy systems with dynamic heterogeneity.
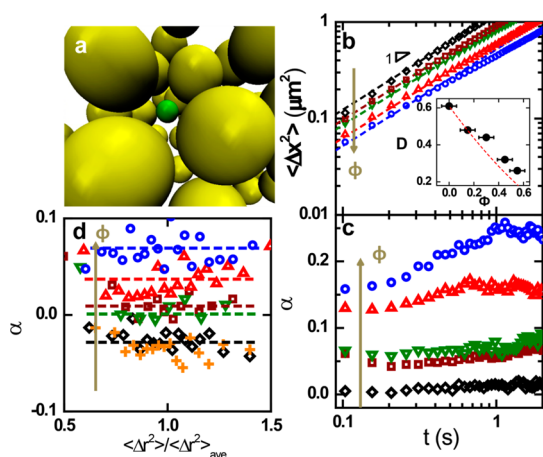
Figure 1. The experimental system. (a) Schematic illustration of small fluorescent probe particles diffusing among larger matrix particles, both of them index and density matched to the solvent. The size ratio is 1:8. **(b)** Mean-squared displacement of the probe plotted against time on log−log scales at matrix volume fraction ϕ = 0, 0.15, 0.30, 0.45, and 0.55, from top to bottom. From the dashed lines, D is inferred from the equation $\langle \Delta x^2 \rangle = 2Dt$. (Inset) D, units of μm^2/s, is plotted against ϕ. The red curve, $D = D_0(1 − \phi)^{1.5}$, is a theoretical prediction taking into account the size difference between probe and matrix particles.[29] The error bars show the uncertainty in measuring absolute volume fraction due to the possible interparticle interaction being less than ideal hard spheres. The error bars of the ordinate are less than the symbol size. **(c)** Non-Gaussian parameter, $\alpha = ((\langle \Delta x^4 \rangle)/(3\langle \Delta x^2 \rangle^2) − 1)$, plotted against time for five values of ϕ. **(d)** Non-Gaussian parameter plotted against particle mobility. The subpopulations of particles are binned based on time-averaged displacement over $\langle \Delta t \rangle$ = 0.1 s. Dashed line is a guide to the eye. "+" is from the simulated Gaussian trajectory. 0%, black diamonds; 15%, brown squares; 30%, green upside-down triangles; 45%, red triangles; 55%, blue circles.

Diffusion of this sort is common in nature and technology. Examples include water diffusing through sand beds (a geology problem),[14] solvents diffusing through polymer gels (a materials problem),[15] and carbon diffusing through steel (a metallurgy problem).[16] A vast theoretical and experimental literature on diffusion and hydrodynamics focuses on the effective diffusivity.[17−26] To the best of our knowledge, these prior studies did not address the displacement distributions that are of primary concern here.

RESULTS

Figure 1a shows a schematic representation of the experiment. We embedded trace quantities of fluorescent poly(methyl methacrylate) (PMMA) particles ($\sim$0.001% volume fraction, $\sim$0.28 μm diameter labeled with rhodamine dye, purchased from Edinburgh Research & Innovation Ltd.) within a matrix of PMMA particles that were optically transparent ($\sim$2.2 μm diameter, same source), suspended in the standard solvent mixture of cyclohexyl bromide and decalin to achieve index-matching and density-matching.[27] Seeking to come as close as possible to a fluid with hard-sphere interactions, we included 1 mg mL^{-1}
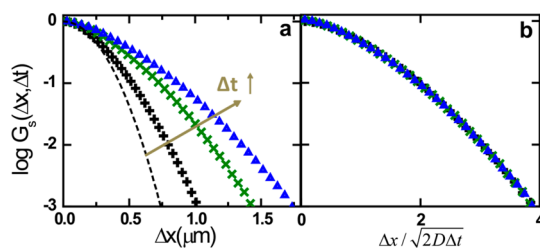

Figure 2. How the displacement probability distribution scales with time. (a) Displacement probability distributions over 3 orders of magnitude plotted logarithmically against displacement, Δx, with ordinate normalized to the maximum, at a volume fraction of 0.45, at times 0.1, 0.2, and 0.3 s. Dashed line is a Gaussian fit to the small displacements at 0.1 s. **(b)** The same ordinate as left, plotted against $\Delta x/(2D\Delta t)^{1/2}$, where D is the diffusivity from the slope of the mean-squared displacement *versus* time and the area under each curve is normalized to unity. Note the collapse of the data.

tetrapentylammonium chloride to screen residue charges on the particles, which gives a Debye length of $\sim$0.1 μm.[10,11] Fluorescence images were taken in epifluorescence mode at room temperature on a Zeiss observer.Z1 microscope with 63$\times$ air objective, using an EMCCD camera (Andor iXon) and data acquisition at 20 frames per second. Using home-developed software[28] the resolution of particle position was <30 nm. Five matrix volume fractions (ϕ) were studied: ϕ = 0, 0.15, 0.30, 0.45, and 0.55.

A typical raw data set amounted to about a million tracer positions as a function of time from $\sim$15 000 particles at each ϕ. The mean squared displacement (MSD) is shown in Figure 1b, plotted on log−log scales against delay time. One sees that initially it is proportional to delay time, but the slope lessens slightly starting at $\sim$1 s, on the order of a few collisions between tracer and the matrix as the tracer moves through interstitial space between matrix particles, whereas Fickian diffusion where MSD is strictly linear with delay time is observed when the tracer particles diffuse in pure solvent. The implied transition length is consistent with the surface distance between matrix particles (see Table S1 of the Supporting Information). The diffusion coefficient was calculated as $\langle \Delta x^2 \rangle = 2Dt$ in the linear regime, where Δx is displacement in a given time interval and the brackets denote time-average and ensemble-average. This was slightly less than in pure solvent (inset of Figure 2b), in qualitative agreement with theoretical predictions taking into account the size difference between probe and matrix particles.[29]

As this large data set included information about fluctuations about the averages, next the non-Gaussian parameter was calculated, $\alpha = (\langle \Delta x^4 \rangle/3\langle \Delta x^2 \rangle^2) − 1$. Plotting this against time (Figure 1c), one observes that α = 0 within experimental uncertainty in pure solvent; α > 0 otherwise; α increases with ϕ; and α is nearly constant over the time window. It is true that non-Gaussian behavior is seen in glassy and supercooled

liquid systems, but those systems are fundamentally different because they display a splitting of mobility between different subpopulations, which is called dynamic heterogeneity.[30−33] Here we observe no such split of mobility (Figure S2 of the Supporting Information). We calculated the non-Gaussian parameter for subpopulations separated according to their different mobility; α was the same regardless of mobility of that subpopulation, suggesting that this splitting-mobility hypothesis could not explain the data (Figure 1d). Trivially, the α values of subpopulations were smaller than those of the ensemble because the former presented a narrower displacement distribution. This we confirmed by simulating trajectories with strictly Gaussian statistics. Also, the non-Gaussian parameter in our system has a small value of ∼0.1−0.3, whereas for glassy systems it is typically ∼1−6, an order of magnitude larger.

This data set was large enough to evaluate the full displacement distribution, including rare events, evaluated over three decades of probability. First, consider obstacles presented by the matrix at $\phi = 0.45$. Figure 2a shows relative probability plotted logarithmically against displacement, evaluated for various time lags. The full distributions show consistent deviations from Gaussian but lack any tendency to show an exponential tail of displacement distribution, differing from the pattern typical for supercooled liquids, which is Gaussian at small displacements and exponential at large displacements.[33,34] Strikingly, they collapse with normalized displacement $\Delta x' = \Delta x/(2Dt)^{1/2}$, consistent with their Fickian displacement.

These distributions, broader than Gaussian, are compared for different volume fraction in Figure 3a, which compares distributions as a function of the respective $\Delta x'$ with the area under each curve normalized to unity. In pure solvent, perfect Gaussian behavior was observed. For stricter comparison to Gaussian behavior, the data were normalized to the Gaussian curve. Plotting this ratio against $\Delta x'$ on a linear scale (Figure 3b), one sees more explicitly that discrepancies were most pronounced for the largest displacements, those displacements whose probability was lowest. It is noteworthy that the displacement distributions deviate from Gaussian behavior already at $\phi = 0.15$, which traditionally would be considered dilute. Given that the matrix may crystallize at $\phi = 0.55$,[35,36] one might expect this to interfere, but we see no significant change in nanoparticle diffusivity nor a split of mobility into fast and slow subpopulations at this concentration (Figure S2 of the Supporting Information). One possible explanation is that the actual concentration is less than this; it is reported that the absolute value of ϕ can shift ±3−6% in this system.[10,11] Regardless of why, this volume fraction presents simply a systematic extension of tendencies already apparent when the matrix concentration is less. Further, there is no suggestion of
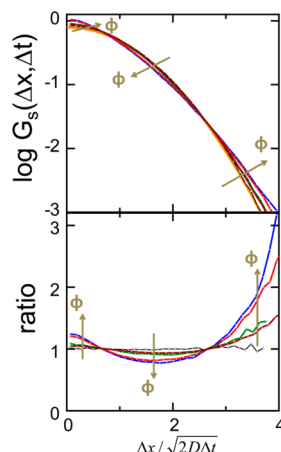

Figure 3. Dependence on volume fraction. (Top) Displacement distributions plotted logarithmically against displacement normalized by $(2D\Delta t)^{1/2}$ at $\Delta t = 0.2$ s for different volume fractions of matrix particles: $\phi = 0$ (black), 0.15 (brown), 0.30 (green), 0.45 (red), and 0.55 (blue), compared to Gaussian distribution (orange line), $(2/\pi)^{1/2}\,e^{-x^2/2}$. Area under each curve is normalized to 1. (Bottom) For each volume fraction, the ratio of the observed probability distribution to the Gaussian is plotted against normalized displacement.

lack of equilibration, as neither aging nor change of nanoparticle mobility is seen over the course of the observation (Figure S3 of the Supporting Information). Deviations from Gaussian are more prominent with increasing ϕ, however. Note also the curious feature that all curves appear to intersect at the same two values of $\Delta x'$, although no interpretation of this empirical observation is offered at this time.

Physically, the greater heterogeneity suggested by the broader distribution of displacement could reflect local obstacle concentrations that differ from the average ϕ according to the local configurations of matrix particles. This is why, reflecting locally relatively crowded and sparse obstacles, we would observe more small displacements and large displacements than Gaussian; the fewer intermediate-sized displacements would then be a consequence of normalizing the area of distribution to unity. These trends become more pronounced with increasing ϕ. Such heterogeneity was supported by further analysis. First, individual trajectories were inspected. Their time-averaged mean square displacement was also found to become increasingly heterogeneous with ϕ (Figure S2 of Supporting Information). Second, adjacent steps in time were found to be correlated in magnitude; that is, large steps were likely to be followed by large steps and *vice versa*. This gave a U-shaped conditional displacement magnitude after a given displacement, centering around zero displacement. This trend grew systematically with increasing ϕ, whereas in pure solvent this bias was not observed (Figure S4 of the Supporting Information). In the course of this study, we reanalyzed already-published data from this laboratory[1,2] and found the same qualitative trend of the conditional displacement,

although the analysis was not made at the time of those publications about other systems that are Fickian yet non-Gaussian.

Matrix particles diffused slowly in this experiment (Supporting Information, Movie S2) but were not immobile as in systems with quenched disorder.[37,38] Then it is reasonable to expect that the smaller tracer particles experienced spatially varying environments, the latter fluctuating more slowly. Given that tracer particles diffused only a fraction of the matrix particle size over the experimental time window, the local environment experienced by different tracer particles differed from point to point according to the random arrangement and the local hydrodynamics of the slowly fluctuating matrix particles. Static obstacles on surfaces have shown to produce anomalous dynamics in 2D,[8,9] and the current system shares these features qualitatively in 3D. It seems that the observed non-Gaussian displacement distributions essentially reflect heterogeneity not averaged out on the time and length scales that we study.

DISCUSSION

Though non-Gaussian diffusion is sometimes identified in supercooled or glassy systems,[30−34] the accepted view of glassy behavior seems to differ significantly. In the trajectories of particles in glassy systems, it is common to analyze the persistence and exchange times (here, the persistence time is the first-passage time for a given particle and exchange time is the waiting time for subsequent passage), and it is found that they decouple typically.[39] The persistence and exchange time distributions in this system, plotted against time lag in Figure 4 (top), display no decoupling. In fact, these two distributions appear to be strictly identical, as one sees from their ratio plotted against time in Figure 4 (bottom).

We now compare our data to the popular continuous time random walk (CTRW) and fractional Brownian motion (FBM) models to describe anomalous diffusion.[40,41] Recently, velocity correlation functions have been suggested to distinguish these processes. We observe a velocity anticorrelation at short time calculated from frame-based displacement correlation, contrasting to unbounded CTRW predictions that do not show negative values due to the absence of correlation between different jumps (Figure S1 of the Supporting Information). It is true that we find certain dynamics features consistent with FBM models: first, the slight velocity anticorrelation at short time; distribution of the ergodicity breaking parameter centered around 1, which is an indicator of the individual particle mobility (Figures S1, S2 of the Supporting Information). However, FBM models require a Hurst exponent less than 0.5 to yield velocity anticorrelation, which simultaneously leads to subdiffusion with an MSD exponent of less than 1, contrasting the Fickian diffusion we
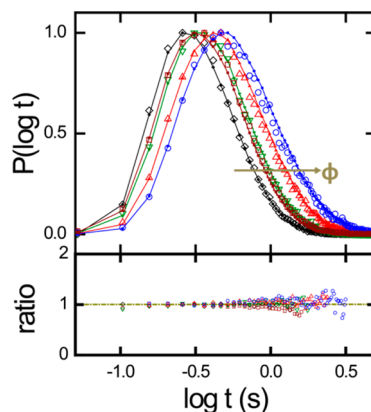

Figure 4. Persistence and exchange time analysis. Top panel: distribution of persistence (solid) and exchange (open) times, compared for $\phi = 0$ (black), 0.15 (brown), 0.30 (green), 0.45 (red), and 0.55 (blue). Threshold distance d is set to 1 μm. No decoupling was seen for $d = 0.5 - 5$ μm. Lines are guides to the eye. Bottom panel: ratio of the distribution of persistence to exchange time at each time lag, plotted with a cutoff of $P(\log t) > 0.05$. Dashed line denoting a ratio of 1 is shown for comparison.

characterized here with MSD linearly growing with time. Physically, the assumptions in CTRW or FBM models are not validated in the current system, however. We do not observe the trapping and discrete jumps in dynamics assumed in CTRW models. We do not observe the memory effects assumed in FBM models.

CONCLUSIONS

The novelty of the present experiments is to demonstrate non-Gaussian yet Fickian diffusion in a very simple system, with physical interactions much simpler than the somewhat esoteric previous systems (actin networks, phospholipid tubules, vesicles), in which this pattern was earlier identified.[1,2] Here the mechanism is probably that hydrodynamics experienced by diffusing particles differs from spot to spot as recognized qualitatively long ago[12,13] without exploring how this would modify the probability distribution of displacement and how the slowly varying local hydrodynamics due to the slowly fluctuating matrix perturbs diffusion. The degree of heterogeneity characterized here lies between one extreme of the simplest fluid of all (no matrix obstacles, $\phi = 0$) and the other extreme of harsh obstacle obstructions (supercooled liquids and glasses). Our observations of more frequent large steps than the Gaussian assumption can be expected to influence the outcome of events whose essence lies in their rarity: dynamics determined by first-passage time, rare-event-initiated chain reactions, diffusion-limited reaction, triggering, and signaling. The phenomenology reported here can be expected to be general, as colloidal suspensions are so common.

The new findings presented here underscore the prominence of non-Gaussian diffusion despite linear mean square displacement. While to observe this in

our crowded situation of highest volume fraction may be easy to understand physically, we emphasize that the tendency starts even when the volume fraction is so low that it might reasonably be considered dilute and expected to follow Gaussian dynamics. The findings underscore, in agreement with recent studies of more esoteric soft matter systems, the seeming ubiquity of non-Gaussian yet Fickian diffusion. This physical situation was previously considered by much earlier analysis of effective diffusivity,[17−26] but this literature did not address theoretically the displacement distributions that are of primary concern here, and the single-particle data presented here were inaccessible to experimentalists at that time. We interpret these results as finding new life in this problem.

METHODS

Trace amounts, ∼0.001% in volume fraction, of fluorescent PMMA particles 0.28 μm in diameter (purchased from Edinburgh Research & Innovation Ltd.) were dispersed evenly into nonfluorescent PMMA particles 2.2 μm in diameter, in a suspension medium of an index-matched and density-matched mixture of cyclohexyl bromide (98%, Aldrich) and decalin (99%, Aldrich), with 1 mg/mL tetrapentylammonium chloride added to screen residual charge between particles. The sample cell was assembled using coverslips as spacers sandwiched between a glass slide and an imaging coverslip. First, the particles were centrifuged in nearly density-matched solvent to achieve a random close packing of ∼64%; then they were diluted with the density-matched solvent mixture to the desired lesser volume fraction. Samples of 0%, 15%, 30%, 45%, and 55% in volume fraction were used in this study. The colloidal dispersion was inserted into the sample cell through an inlet hole drilled through the glass slide and rapidly sealed with a molten mixture of galactose and dextrose (1:1). The sample was allowed to equilibrate on the microscope stage for a few hours, and epifluorescence microscopy imaging was carried out at a focal plane at least 30 μm away from the surface. Spatial resolution of ∼30 nm was achieved using a 63× air objective (NA = 0.75) with 1.6× postmagnification and image analysis software written in-house.

Conflict of Interest: The authors declare no competing financial interest.

Supporting Information Available: Details on comparison with CTRW and FBM models (Figures S1 and S2), estimates of time scales, movies taken with a fluorescence microscope to show probe and matrix dynamics. This material is available free of charge *via* the Internet at http://pubs.acs.org.

REFERENCES AND NOTES

1. Wang, B.; Kuo, J.; Bae, S. C.; Granick, S. When Brownian Diffusion Is Not Gaussian. *Nat. Mater.* **2012**, *11*, 481–485.
2. Wang, B.; Anthony, S. M.; Bae, S. C.; Granick, S. Anomalous yet Brownian. *Proc. Nat. Acad. Sci. U.S.A.* **2009**, *106*, 15160–15164.
3. Skaug, M. J.; Mabry, J.; Schwartz, D. K. Intermittent Molecular Hopping at the Solid-Liquid Interface. *Phys. Rev. Lett.* **2013**, *110*, 256101.
4. Yu, C.; Guan, J.; Chen, K.; Bae, S. C.; Granick, S. Single-Molecule Observation of Long Jumps in Polymer Adsorption. *ACS Nano* **2013**, *7*, 9735–9742.
5. Kurtuldu, H.; Guasto, J. S.; Johnson, K. A.; Gollub, J. P. Enhancement of Biomixing by Swimming Algal Cells in Two-Dimensional Films. *Proc. Nat. Acad. Sci. U.S.A.* **2011**, *108*, 10391–10395.
6. Kim, J.; Kim, C.; Sung, B. J. Simulation Study of Seemingly Fickian but Heterogeneous Dynamics of Two Dimensional Colloids. *Phys. Rev. Lett.* **2013**, *110*, 047801.
7. Goohpattader, P. S.; Chaudhury, M. K. Diffusive Motion with Nonlinear Friction: Apparently Brownian. *J. Chem. Phys.* **2010**, *133*, 024702.
8. He, K.; Khorasani, F. B.; Retterer, S. T.; Thomas, D. K.; Conrad, J. C.; Krishnamoorti, R. Diffusive Dynamics of Nanoparticles in Arrays of Nanoposts. *ACS Nano* **2013**, *7*, 5122–5130.
9. Skinner, T. O. E.; Schnyder, S. K.; Aarts, D. G. A. L.; Horbach, J.; Dullens, R. P. A. Localization Dynamics of Fluids in Random Confinement. *Phys. Rev. Lett.* **2013**, *111*, 128301.
10. Royall, C. P.; Poon, W. C. K.; Weeks, E. R. In Search of Colloidal Hard Spheres. *Soft Matter* **2013**, *9*, 17–27.
11. Poon, W. C. K.; Weeks, E. R.; Royall, C. P. On Measuring Colloidal Volume Fractions. *Soft Matter* **2012**, *8*, 21–30.
12. Ando, T.; Skolnick, J. Crowding and Hydrodynamic Interactions Likely Dominate in Vivo Macromolecular Motion. *Proc. Nat. Acad. Sci. U.S.A.* **2010**, *107*, 18457–18462.
13. Guo, G.; Liu, G.; Thompson, K. E. Numerical Analysis of the Effects of Local Hydrodynamics on Mass Transfer in Heterogeneous Porous Media. *Chem. Eng. Commun.* **2003**, *190*, 1641–1660.
14. Badv, K.; Faridfard, M. R. Laboratory Determination of Water Retention and Diffusion Coefficient in Unsaturated Sand. *Water Air Soil Pollut.* **2005**, *161*, 25–38.
15. Andersson, D.; Engberg, D.; Swenson, J.; Svanberg, C.; Howells, W. S.; Borjesson, J. Diffusive Solvent Dynamics in a Polymer Gel Electrolyte Studied by Quasielastic Neutron Scattering. *J. Chem. Phys.* **2005**, *122*, 234905.
16. Simonovic, D.; Ande, C. K.; Duff, A. I.; Syahputra, F.; Sluiter, M. H. F. Diffusion of Carbon in bcc Fe in the Presence of Si. *Phys. Rev. B* **2010**, *81*, 054116.
17. Mu, D.; Liu, Z.-S.; Huang, C.; Djilali, N. Prediction of the Effective Diffusion Coefficient in Random Porous Media Using the Finite Element Method. *J. Porous Mater.* **2007**, *14*, 49–54.
18. Moreno, A. J.; Colmenero, J. Relaxation Scenarios in a Mixture of Large and Small Spheres: Dependence on the Size Disparity. *J. Chem. Phys.* **2006**, *125*, 164507.
19. Weissberg, H. L. Effective Diffusion Coefficient in Porous Media. *J. Appl. Phys.* **1963**, *34*, 2636–2639.
20. Kluijtmans, S. G. J. M.; Philipse, A. P. First in Situ Determination of Confined Brownian Tracer Motion in Dense Random Sphere Packings. *Langmuir* **1999**, *15*, 1896–1898.
21. Kim, I. C.; Torquato, S. Diffusion of Finite-Sized Particles in Porous Media. *J. Chem. Phys.* **1992**, *96*, 1498–1503.
22. Chang, R.; Jagannathan, K.; Yethiraj, A. Diffusion of Hard Sphere Fluids in Disordered Media: A Molecular Dynamics Simulation Study. *Phys. Rev. E* **2004**, *69*, 051101.
23. Saxton, M. J. Wanted: A Positive Control for Anomalous Subdiffusion. *Biophys. J.* **2012**, *103*, 2411–2422.
24. Bourg, I. C.; Sposito, G. Connecting the Molecular Scale to the Continuum Scale for Diffusion Processes in Smectite-Rich Porous Media. *Environ. Sci. Technol.* **2010**, *44*, 2085–2091.
25. Zhao, Q.; Papadopoulos, P. Modeling and Simulation of Liquid Diffusion through a Porous Finitely Elastic Solid. *Comput. Mech.* **2013**, *52*, 553–562.
26. Batchelor, G. K. Brownian Diffusion of Particles with Hydrodynamic Interaction. *J. Fluid Mech.* **1976**, *74*, 1–29.
27. Wiederseiner, S.; Andreini, M.; Epely-Chauvin, G.; Ancey, C. Refractive-Index and Density Matching in Concentrated Particle Suspensions: A Review. *Exp. Fluids* **2011**, *50*, 1183–1206.

28. Anthony, S. M.; Granick, S. Image Analysis with Rapid and Accurate 2D Gaussian Fitting. *Langmuir* **2009**, *25*, 8152–8160.

29. Douglas, J. F.; Leporini, D. Obstruction Model of the Fractional Stokes-Einstein Relation in Glass-Forming Liquids. *J. Non-Cryst. Solids* **1998**, *235−237*, 137–141.

30. Weeks, E. R.; Crocker, J. C.; Levitt, A. C.; Schofield, A.; Weitz, D. A. Three-Dimensional Direct Imaging of Structural Relaxation Near the Colloidal Glass Transition. *Science* **2000**, *287*, 627–631.

31. Kegel, W. K.; van Blaaderen, A. Direct Observation of Dynamical Heterogeneities in Colloidal Hard-Sphere Suspensions. *Science* **2000**, *287*, 290–293.

32. Hedges, L. O.; Jack, R. L.; Garrahan, J. P.; Chandler, D. Dynamic Order-Disorder in Atomistic Models of Structural Glass Formers. *Science* **2009**, *323*, 1309–1313.

33. Chaudhuri, P.; Berthier, L.; Kob, W. Universal Nature of Particle Displacements Close to Glass and Jamming Transitions. *Phys. Rev. Lett.* **2007**, *99*, 060604.

34. Mandal, S.; Chikkadi, V.; Nienhuis, B.; Raabe, D.; Schall, P.; Varnik, F. Single-Particle Fluctuations and Directional Correlations in Driven Hard-Sphere Glasses. *Phys. Rev. E* **2013**, *88*, 022129.

35. Royall, C. P.; Louis, A. A.; Tanaka, J. Measuring Colloidal Interactions with Confocal Microscopy. *J. Chem. Phys.* **2007**, *127*, 044507.

36. Yethiraj, A.; van Blaaderen, A. A Colloidal Model System with an Interaction Tunable from Hard Sphere to Soft and Dipolar. *Nature* **2003**, *421*, 513–517.

37. Kurzidim, J.; Coslovish, D.; Gerhard, K. Dynamic Arrest of Colloids in Porous Environments: Disentangling Crowding and Confinement. *J. Phys.: Condens. Matter* **2011**, *23*, 234122.

38. Kim, K.; Miyazaki, K.; Saito, S. Slow Dynamics, Dynamic Heterogeneities, and Fragility of Supercooled Liquids Confined in Random Media. *J. Phys.: Condens. Matter* **2011**, *23*, 234123.

39. Hedges, L. O.; Maibaum, L.; Chandler, D.; Garrahan, J. P. Decoupling of Exchange and Persistence Times in Atomistic Models of Glass Formers. *J. Chem. Phys.* **2007**, *127*, 211101.

40. Burov, S.; Jeon, J.-H.; Metzler, R.; Barkai, E. Single Particle Tracking in Systems Showing Anomalous Diffusion: the Role of Weak Ergodicity Breaking. *Phys. Chem. Chem. Phys.* **2011**, *13*, 1800–1812.

41. Magdziarz, M.; Weron, A.; Burnecki, K.; Klafter, J. Fractional Brownian Motion Versus the Continuous-Time Random Walk: A Simple Test for Subdiffusive Dynamics. *Phys. Rev. Lett.* **2009**, *103*, 180602.